

## Mineralogy of the Grès de Thiviers (northern Aquitaine, France)

ALESSANDRO SEMPIO and ALESSANDRO F. GUALTIERI\*

Dipartimento di Scienze della Terra, Università degli Studi di Modena e Reggio Emilia, 41100 Modena, Italy

Submitted, October 2001 - Accepted, March 2002

**ABSTRACT.** — This paper reports the mineralogical characterisation of the *Grès de Thiviers* (GT), a unique natural pigment used in the industry of traditional tile ceramics. The only occurrence of this raw material, composed of quartz and goethite, is a small region in the SW of France where it is exploited and exported to the European and Far East markets. GT is mainly used as a bulk red pigment for white stoneware and its stability in firing is a direct consequence of the unique nature. In fact, despite the nature of the raw materials composing the ceramic mixture and their behaviour at high temperature, GT invariably yields a final red colour to the fired ceramic body. The stability stems from the fact that goethite (yellow colour) which later transforms into hematite (red colour) is the cement of quartz grains. Thus, in firing, because of the protective shield formed by the inert quartz grains, the newly-formed hematite crystals do not get in contact with other reacting phases such as the alkaline glass and retain the red colour (Sempio and Gualtieri, 2001).

The mineralogy of the GT deposits was described in the light of the peculiar genesis and chemical variability. In fact, GT occurrence is closely related to the karstic system permeating the late Cretaceous limestone in this region. According to the different formation environment it was possible to describe

the four typical GT textures: laminar, oolitic, dendritic, and homeoblastic.

GT samples contain amorphous substance with composition  $[\text{SiO}_2 + \text{Fe}_2\text{O}_3 \text{ or } \text{FeO}(\text{OH})]$  which is the colloidal precursor of the crystalline phases quartz and goethite.

**RIASSUNTO.** — In questo lavoro vengono descritte le caratteristiche mineralogiche del Grès de Thiviers, un materiale naturale proveniente da una zona della Francia sud occidentale compresa fra le regioni del Périgord e della Charentes ed utilizzato come pigmento da massa per ceramiche tradizionali quali il grès porcellanato. La semplice composizione mineralogica (quarzo e goethite) nasconde in realtà caratteristiche tessiturali uniche al mondo e responsabili delle peculiari proprietà fisico-chimiche e della stabilità del colore in fase di cottura.

I campioni investigati sono rappresentativi dei quattro tipi diversi di tessiture osservati per il GT: laminare, oolitica, dendritica e omeoblastica ed hanno permesso di mettere in relazione la tessitura con le caratteristiche mineralogiche. In particolare è stato possibile riconoscere attraverso analisi quantitativa in diffrazione di raggi X con il metodo Rietveld-R.I.R. la presenza di fase amorfa, precursore non cristallizzato di quarzo e goethite. Fra i minerali secondari, sono stati osservati caolinite, calcite, ematite ed una fase argillosa a 15 Å probabilmente *nontronite*.

Questo studio può essere molto utile per l'attività

\* Corresponding author, E-mail: alex@unimo.it

estrattiva in quanto indica chiaramente quali sono le tessiture ed i tipi di materiale con le migliori caratteristiche per le applicazioni industriali.

KEY WORDS: *Grès de Thiviers, goethite, quartz, Rietveld, amorphous phase, texture.*

## INTRODUCTION

This work deals with the characterization of the Grès de Thiviers (GT), a unique natural pigment used in the industry of traditional ceramics. The only occurrence of this raw material is the Aquitaine region in the SW of France, where it is exploited, worked and exported in the European and Far East markets. GT is mainly composed of quartz, goethite and minor phases such as hematite, calcite and clay minerals.

The coloring properties of the GT rocks are well known since the prehistoric age. As a matter of fact, this region is a very famous archaeological site famous for the Lascaux caves with the famous Neolithic mural paintings. The images of animals reproduced on the cave walls were realized during the Paleolithic age using natural pigments such as GT mixed with animal fats (Dornieden *et al.*, 2000; Gersal, 1998; Masset, 1997) and water. The yellow color was obtained with goethite rich mixtures whereas red color was obtained with hematite rich mixtures (probably calcined goethite). This «raw material» is still used as pigment added to mixtures for the production of red stoneware ceramics. The peculiar nature of GT is responsible for the properties of this natural pigment in firing. The addition to a common mixture for traditional floor tile ceramics (mainly a ternary mixture composed of kaolinite-quartz-feldspar) fired at 1200-1250 °C produces a final red color as a result of the goethite [ $\alpha$ -FeO(OH)] transformation to hematite [ $\alpha$ -Fe<sub>2</sub>O<sub>3</sub>]. The success of this natural pigment is the stability of the colour under extremely different conditions: different mixture composition, different firing cycles, different technological processes (Sempio and Gualtieri, 2001).

From a geological point of view, Northern Aquitaine is characterized in general by Jurassic and Cretaceous limestone formations possibly containing iron-rich formations of limited occurrence. There are two iron-rich associations present in the Aquitaine regions of Périgord and Charentes. The first one consists of deposits related to pedogenetic processes taking place during the warm Tertiary and the moderate Quaternary paleoclimates (Gourdon-Platel, 1977). They are widely distributed on a regional scale, with quartz and clay minerals cemented by iron oxides.

The second one of diagenetic origin is characterized by deposits formed inside sinkholes and/or hollows present in the karstic system of the late-Cretaceous limestones. They appear as a lateritic coverage in associations with a clayey-sandy complex, or in the form of very hard flint rock plates, brownish in color, due to the overlap of a number of millimetric beds constituted by newly-formed quartz crystals. The material is «commercially» called *Grès de Thiviers*, from the name of the village where it was first exploited. Nowadays all the exploited outcrops are approximately located in a region within the Périgord and the Charentes zone (Fig. 1 after Gourdon-Platel, 1977).

In this area, GT does not exist as a continuous formation but the deposits are very limited and discontinuous in space. According to Platel and Dubreuilh (1992), there are different structural modes of occurrence of GT: they could be covered by Tertiary and Quaternary deposits (Fig. 2A-B) or they could be located nearby the surface covered by the recent thin soil deposits (Fig. 2C-E). In both cases, GT appears in the form of big blocks (about 1-10 m) as a result of the mechanical and chemical demolition of even larger blocks embedded in a clayey-sandy matrix (Platel and Dubreuilh, 1992).

The different occurrences are due to the different mechanism of deposition of GT (Dubreuilh 1980, 1982, 1984, 1989; Gourdon-Platel, 1975; Platel 1980, 1981, 1983). In the calcareous substrate, the karstic system engulfed the residual materials produced by the

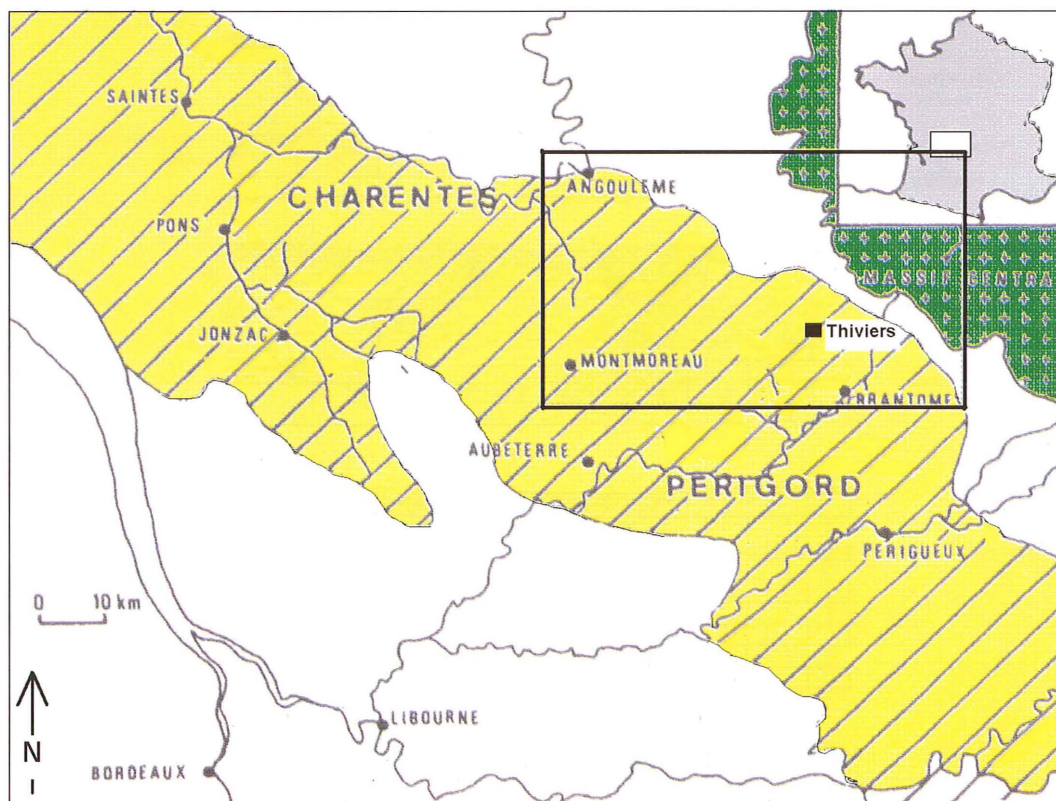


Fig. 1 – Sketch of the localization and geology of the silico-iron sandstone formations of Northern Aquitaine region (after Gourdon-Platel, 1977). Legend: yellow region with 45° lines = Cretaceous limestones; green region with crosses = Crystalline basement.

alteration and the destruction of the continental complex. The shape and size of the hollows can be extremely variable both in diameter and depth (from about 5 to 10 m).

Regarding the origin of the iron rich sediments, it is thought that in the Eocene, a loess deposit covered the calcareous basement, previously interested by the karstic phenomena. Subsequently, these deposits formed inside small underground depressions. The rain waters, permeating the detrital series of the Tertiary continental (siderolitic facies) were saturated in silicic acid and iron and slowly permeated the silt sediments. Collected in correspondence to the hollows where these sediments deposited, waters prompted a

diagenetic process and the crystallization of quartz and goethite was possible where the concentration of silicic acid and eventually Fe oxides reached high levels (Platel and Dubreuilh, 1992).

Concerning the compositional variability, under the same climatic conditions, the quartz and goethite was possible where the concentration of silicic acid and eventually Fe oxides reached high levels (Platel and Dubreuilh, 1992).

Concerning the compositional variability, under the same climatic conditions, the amorphous silica is immediately dispersed in solution in the form of acidic monomers  $\text{Si}(\text{OH})_4$ , in equilibrium with the environment for concentrations of 120 ppm at 25°C and pH < 9. Whenever conditions of saturation of silica are reached, colloidal amorphous silica is formed with a solubility 10 to 20 times larger than quartz. The silica polymerization is crucial to explain the genesis of GT because it

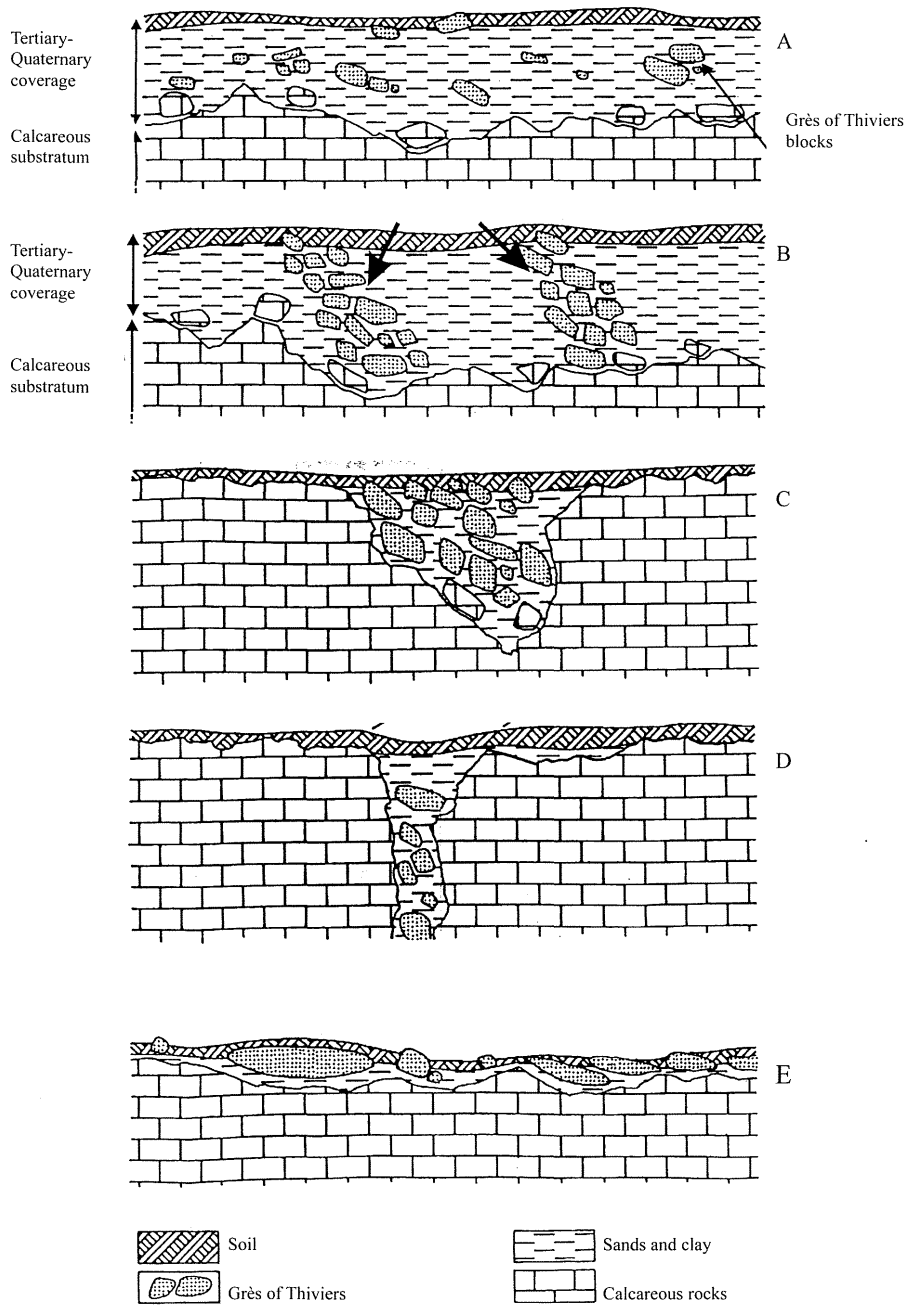


Fig. 2 – Different possible deposits of the Grès di Thiviers: blocks randomly spread (A); randomly concentrated (B); located inside pockets in close relationship with the karstic system (C); in correspondence with linear fractures (D); blocks directly exposed on the ground surface (E) (modified after Platel and Dubreuilh, 1992).

accounts for the high concentration of silica in solution which in turn transformed into quartz during the diagenetic process.

In the present work the description of the GT allowed to disclose the minerogenetic conditions during the diagenetic process. The knowledge of such characteristics is crucial for the mining activity. In fact, the composition of GT is variable and consequently technological properties such as the coloring power (related to the amount of iron oxides and their microstructure) are also variable. Thus, the understanding of the relationship between the mineralogical-textural characteristics and the technological properties is fundamental for the prediction of occurrence and selection of the best material during the mining activity.

## EXPERIMENTAL

### Sampling

The mining activity of the GT is indeed very simple: during the excavation, operators manually select the GT blocks which are separated from the clay and accumulated on the shovel excavator. The clean blocks are stored in containers and transported to the main mining site in special box to divide the different GT qualities. Here, the GT blocks are crushed and grossly milled with the aid of mechanical crushers to select fragments with an average size of around 10-30 mm. This primary product is later finely milled (down to ca. 10-50 mm), packed and commercialised.

A preliminary survey in the region was conducted to collect a number of samples to be analyzed by optical microscopy and to create subgroups of GT samples with specific macroscopic and textural characteristics. The preliminary survey led to the selection of four different representative outcrops in the Périgord and Charentes areas to be further investigated (Fig. 3 – the box of Fig. 1 - with the sampling sites):

(1) *DIRAC - Chez Baudard*: In the wood, an outcrop of about 100 m diameter. The open quarry has a circular shape with a maximum

depth of ca. 5 m. GT coherent blocks are intercalated within the clay matrix. They have irregular form and dimension (from a few cm to some m and are assigned to the type of deposit A of Fig. 2). Under the surface layer, there is another clay layer denominated *white clay* and empirically set as the lower limit of excavation. In this outcrop, we collected samples: CTh1: Compact material with an intense ochre color. These blocks originally belonged to a well-stratified formation; CTh2: The white clay from the lower layer; CTh3: Material with an intense brown color, not layered; CTh4: Calcareous rock block associated with the GT blocks representative of the Upper Cretaceous limestones; CTh5: a sample of the clay that constitutes the matrix of the GT blocks.

2) *TORSAC – La Grande Courrière*: The quarry is located in an open farm soil. It is relatively wide (around 2500 m<sup>2</sup>) with an estimated depth of 8 m. In this site, GT appears less discontinuous with some meso-folded layers about 2 m thick (Type of deposit E in Fig. 2). Here we collected sample CTh6: Compact material with a dark brown tonality.

3) *FOREST D'HORTE - Les Coupes Carrès*: This site is located inside of a dense wood where a preliminary investigation was performed to verify the existence of GT. We assigned this deposit to type C in Fig. 2. Vegetation is abundant and the surface soil is markedly clayey. At variance, GT blocks appear right on the surface. Sample CTh7 is a compact material of ochre color with a well evident stratified microstructure with alternate light and dark layers. In a few CTh7 specimens, a dendritic like mesostructure is also macroscopically observed.

4) *VILLARS - Beis Vieux*: This quarry is currently exploited. In this site, the contact between the white clays and GT layers is evident (Deposit of type B in Fig. 2). The quarry is approximately 2000 m<sup>2</sup> and about 7-8 m deep. Sample CTh8 is homogeneous, very hard and compact with the darkest observed brown tonality.

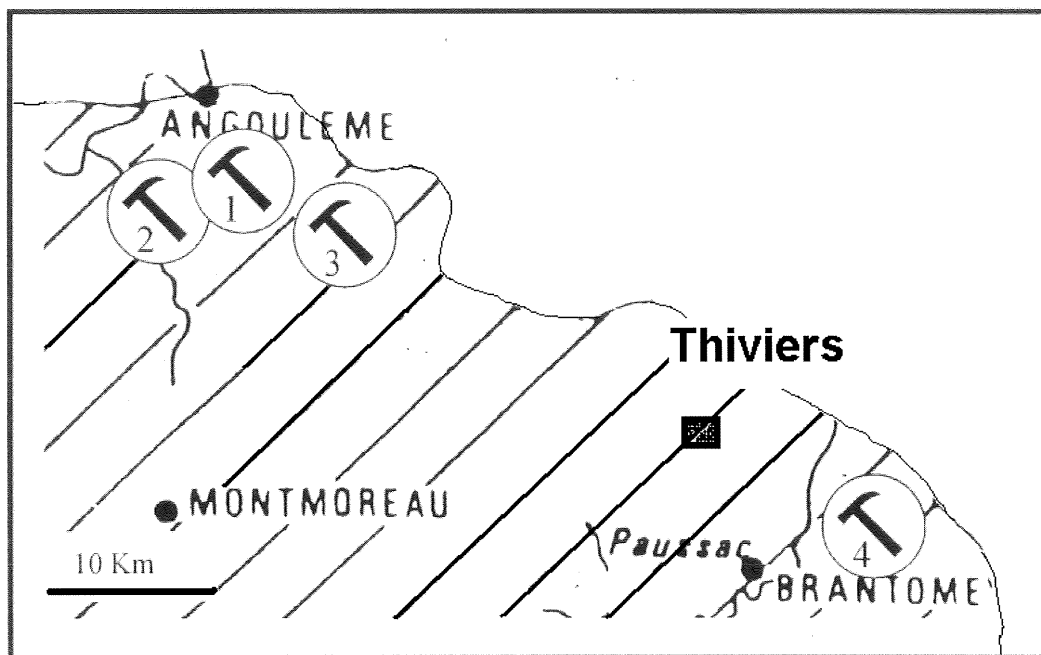


Fig. 3 – Sketch map of the sampling area corresponding to the box reported in Fig. 1.

### *Experimental techniques*

The X-ray fluorescence analyses were obtained using a spectrometer Philips PW1480 and the quantitative analysis was possible by selecting a number of appropriate silicate and oxide standards for the calibration curves. Loss of ignition (L.O.I) was determined by the TGA weight loss at 1000 °C using a SEIKO SSC/5200. The X-ray powder diffraction data were collected with an automatic powder-diffractometer Philips PW3710 in a Bragg-Brentano geometry and a  $\text{CuK}\alpha$  monochromatised radiation. For the qualitative analyses, data were collected in the range 3-60  $^{\circ}2\theta$ , step scan of 0.02  $^{\circ}2\theta$  and 2 s/steps. For the quantitative phase analyses (QPA), 10 wt% Corundum NIST 676 was added to the powder to perform the Rietveld-R.I.R. (Reference Intensity Ratio) combined method (Gualtieri, 2000). Data were collected in the range 10-80  $^{\circ}2\theta$  with step scan of 0.02  $^{\circ}2\theta$  and 15 s/step.

Each data set was refined using GSAS (Larson and Von Dreele, 1994). The starting structure models were taken from the literature and kept fixed during the refinement. The atomic displacement parameters  $U_{\text{iso}}$  were set to the single crystal values for every phase and kept fixed during the refinement procedure. Refinements were carried out using this strategy: a) the background was successfully fitted with a Chebyshev function with a variable number of coefficients depending on its complexity; b) the peak profiles were modelled using a pseudo-Voigt function with one Gaussian and one Lorentzian coefficient; c) The lattice constants, the phase fraction and the coefficients corresponding to the sample displacement and asymmetry were also refined. The cut-off value for the calculation of the peak profiles in all refinements was 0.05%.

For the optical study, GT thin sections both parallel and perpendicular to the stratification direction were prepared and examined using a

transmission microscope with polarized light. SEM observations were performed using a Philips XL40/604 at ca.  $10^{-6}$  torr and a variable tension of 10-25 kV. Samples were coated with a gold layer of 10 nm for morphology and C for chemical analyses in energy dispersive mode (EDS).

## RESULTS

Table 1 reports the chemical analyses of all the samples and the mineralogical quantitative phase analyses of the selected GT samples CTh1, CTh3, CTh6, CTh7, and CTh8.

The final agreement factors of the Rietveld refinements  $R_{wp}$  were all lower than 11%,  $R_p$

all lower than 14%, and  $\chi^2$  all lower than 5.0. The full data sets of the GSAS experimental files of the refinements are available upon request to the corresponding author.

For the CTh1, CTh3, CTh6, CTh7, and CTh8 samples, iron which belongs to goethite and free iron in the system (which belongs to either hematite or amorphous iron hydroxides) was calculated throughout stoichiometric calculations by considering the weight estimates from the QPA. CTh4 sample corresponds to a calcareous rock. Qualitative mineralogical analysis of that sample shows the presence of calcite and quartz. This sample represents a coherent part of the Cretaceous limestone body. As far as the incoherent part is concerned, both clays CTh2 and CTh5 contain

TABLE 1

*X-ray fluorescence chemical analyses of the investigated samples and quantitative phase analyses using the Rietveld-RIR method of selected GT samples.*

	CTh 1	CTh 3	CTh 6	CTh 7	CTh 8	CTh2	CTh5	CTh4
SiO <sub>2</sub>	78.2	84.1	64.8	72.3	95.2	42.7	44.3	3.4
Al <sub>2</sub> O <sub>3</sub>	0.1	0.1	0.1	0.3	0.1	21.1	23.8	0.3
Fe <sub>2</sub> O <sub>3</sub>	18.1	13.2	28.9	22.9	3.2	9.8	10.0	0.3
TiO <sub>2</sub>	0.0	0.0	0.0	0.0	0.0	0.7	0.8	0.0
CaO	0.1	0.1	0.2	0.1	0.0	6.7	2.5	53.3
MgO	0.1	0.1	0.1	0.1	0.1	1.2	1.4	0.4
MnO	0.1	0.1	0.1	0.1	0.1	0.1	0.1	0.1
Na <sub>2</sub> O	0.1	0.1	0.0	0.0	0.0	0.1	0.1	0.3
K <sub>2</sub> O	0.0	0.0	0.0	0.0	0.0	0.9	0.9	0.0
P <sub>2</sub> O <sub>5</sub>	0.2	0.1	0.2	0.1	0.0	0.1	0.0	0.0
L.O.I.	3.0	2.2	5.2	3.8	1.2	16.6	16.0	41.8
TOT	99.9	100.0	99.6	99.7	99.9	100.0	99.9	99.9
Quartz	71.0 (1)	75.2 (1)	54.9 (1)	66.6 (1)	82.2 (1)	—	—	—
Goethite	13.4 (2)	10.5 (2)	19.8 (2)	18.0 (2)	1.6 (1)	—	—	—
Hematite	0.1 (1)	—	0.2 (1)	—	—	—	—	—
Calcite	0.1(1)	0.2 (1)	—	—	—	—	—	—
Amorphous fase	15 (1)	14 (1)	25 (1)	15 (1)	16 (1)	—	—	—
Fe <sub>2</sub> O <sub>3</sub> Goethite	12.1	9.1	17.8	16.2	1.5	—	—	—
Fe <sub>2</sub> O <sub>3</sub> free	6.0	4.1	11.1	6.7	1.7	—	—	—



quartz, hematite, kaolinite and a 15 Å-clay later identified as nontronite for the close similarity of the powder pattern with that reported on the JCPDS data bank (card nr. 340842; Eggleton, 1977). It is important to stress here that the identification of the nontronite phase is merely speculative and that a conclusive attribution should be accomplished by further investigations out of the goals of the present work. Calcite is present only in sample CTh2.

As an example, Fig. 4 depicts the observed and the calculated powder patterns and relative difference curve of the Rietveld refinement performed on CTh1 sample.

The microscopic observation allowed the understanding of the microstructure, texture and morphology relationships existing between the iron hydroxides/oxides and the silica particles.

The collected samples are representative of

all the observed GT textures. Fig. 5 is a gallery of the observed textures. Fig. 5A shows the millimetric beds (laminar texture) forming sample CTh6 composed of well crystallized, sometimes twinned, quartz crystals of nearly 200 µm. In thin section, they show a regular division into concentric zones, characterized by polygonal halos parallel to the crystal faces, of clear and dark color according to the content of the iron oxide (sample CTh1 in Fig. 5B). Fig. 5C depicting sample CTh8, shows another very common texture of GT composed of chalcedony oolites with a diameter of ca. 10-20 µm. Fig. 5D is a typical dendritic texture in sample CTh7 and Fig. 5E is a picture of the homeoblastic texture in sample CTh3.

The image of Fig. 6A is particularly interesting as it shows the morphological relationships existing between the two different phases quartz and goethite. A quartz grain

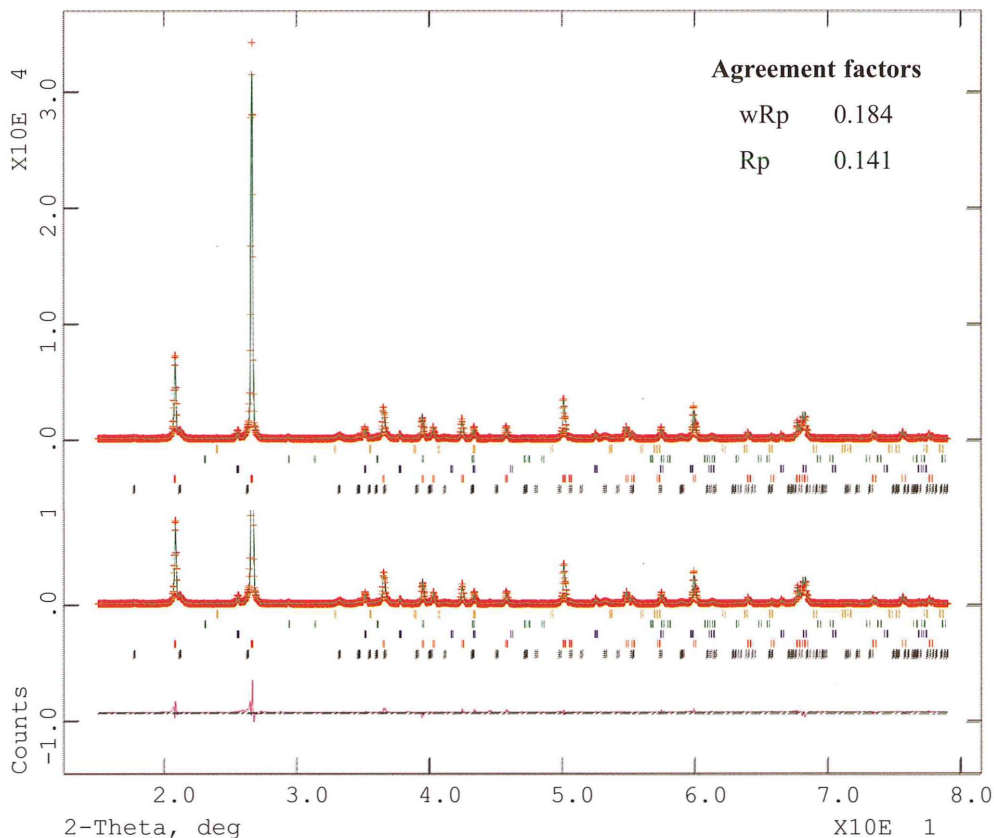
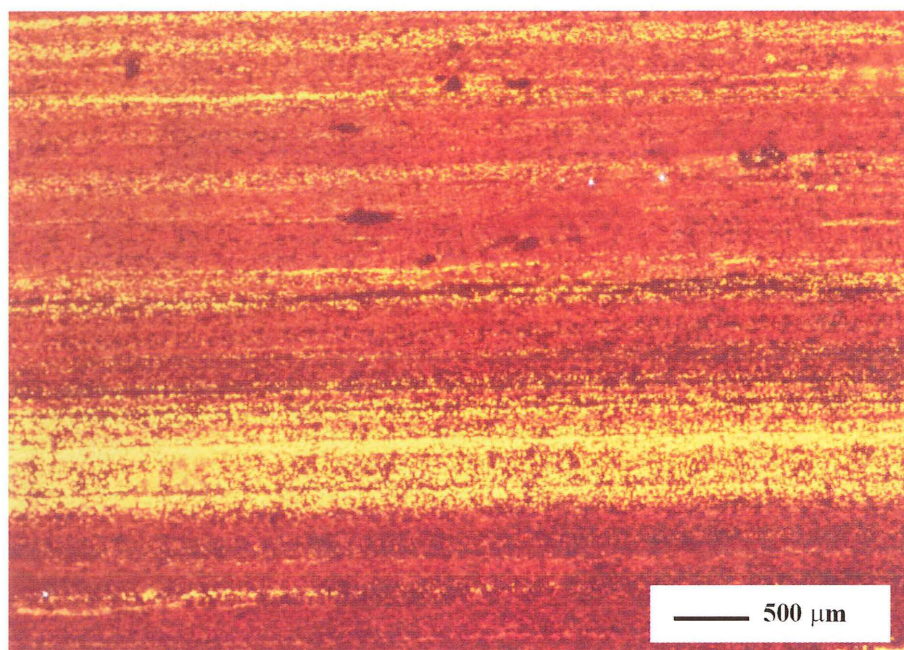
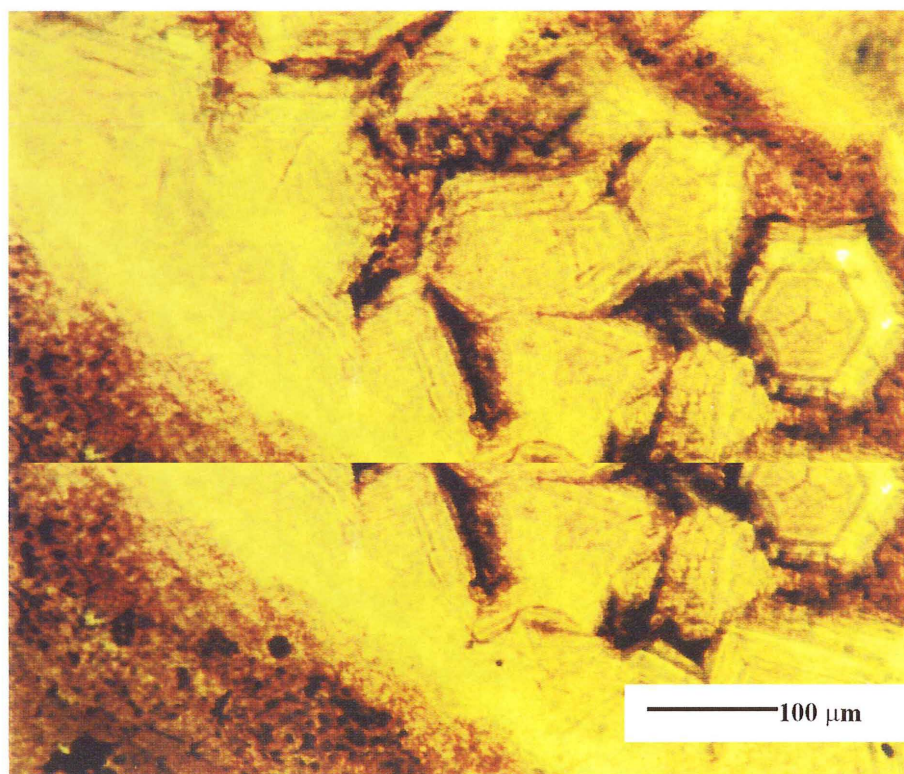


Fig. 4 – The observed and the calculated powder patterns and relative difference curve of the Rietveld refinement performed on CTh1 sample. Markers indicate the reflections of each phase (lines from the bottom: goethite, quartz, corundum NIST 676 as internal standard, calcite, hematite).





A



B

Fig. 5 – Textures of the GT samples: (A) in CTh6 sample, composed of layers of well crystallized, sometimes twinned, quartz crystals (laminar); (B) in CTh1, showing a regular division into concentric zones, characterized by polygonal halos parallel to the crystal faces, of clear and dark color according to the content of the iron oxide (laminar).



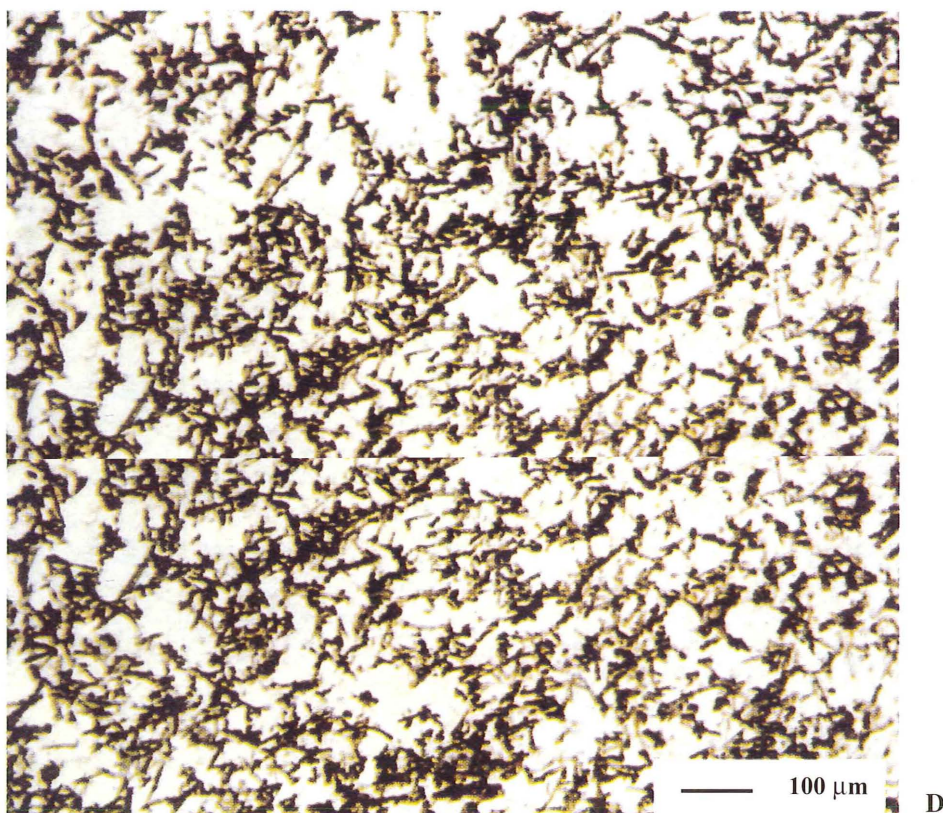
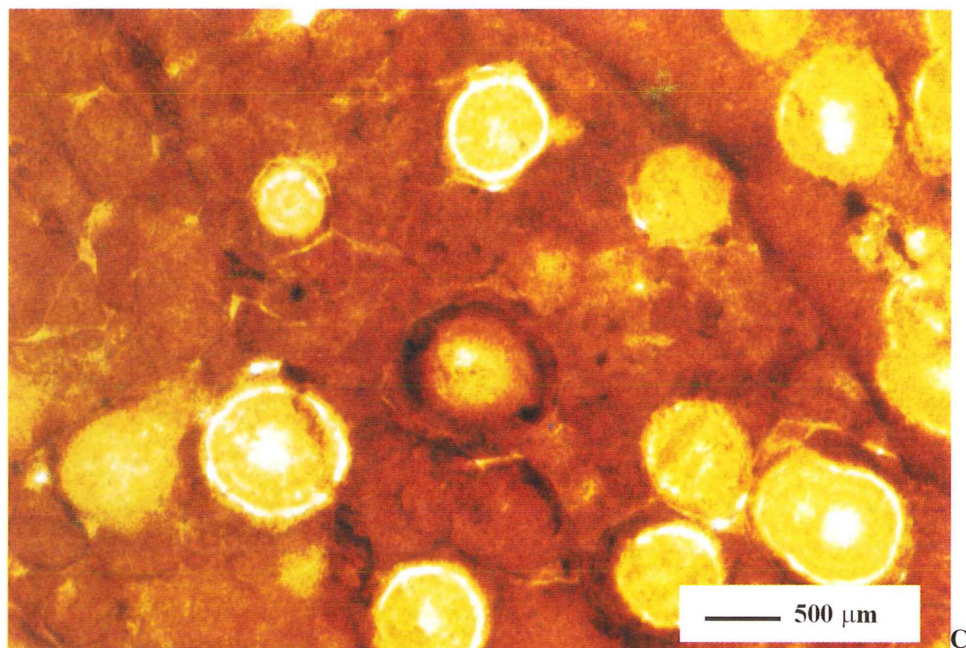


Fig. 5 – (C) in CTh8, composed of chalcedony oolites with a diameter of ca. 10-20  $\mu\text{m}$  (oolitic); (D) in CTh7, dendritic;



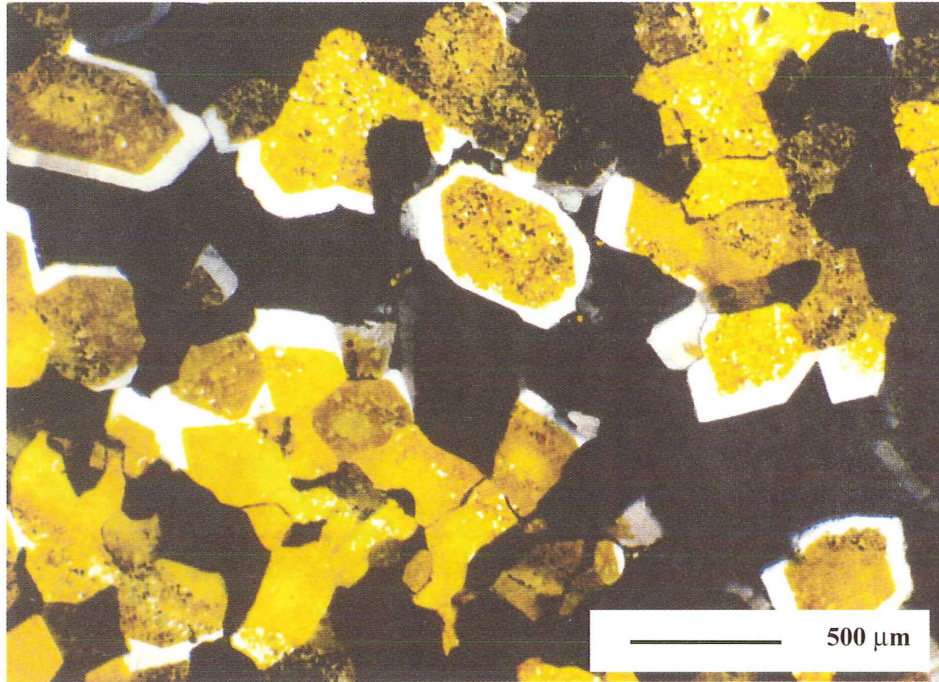


Fig. 5 – (E) in CTh3, homeoblastic.

partly covered by an agglomerate of smaller crystals corresponding to iron oxides. A highly magnified image of the quartz grain evidenced a tiny cavity entrapping small crystal fragments of quartz and iron oxides (Fig. 6B). Besides, in the very same sample, quartz can be found idiomorphic (Fig. 6C) clearly indicating that GT contains both quartz crystals cemented by goethite and idiomorphic non-cemented quartz crystals. Fig. 6D again evidences the peculiar morphology of the quartz aggregates cemented by iron oxides. In the very same sample, quartz can be found idiomorphic (Fig. 6C) clearly indicating that GT contains both quartz crystals cemented by goethite and idiomorphic non-cemented quartz crystals. Fig. 6D again evidences the peculiar morphology of the quartz aggregates cemented by iron oxides.

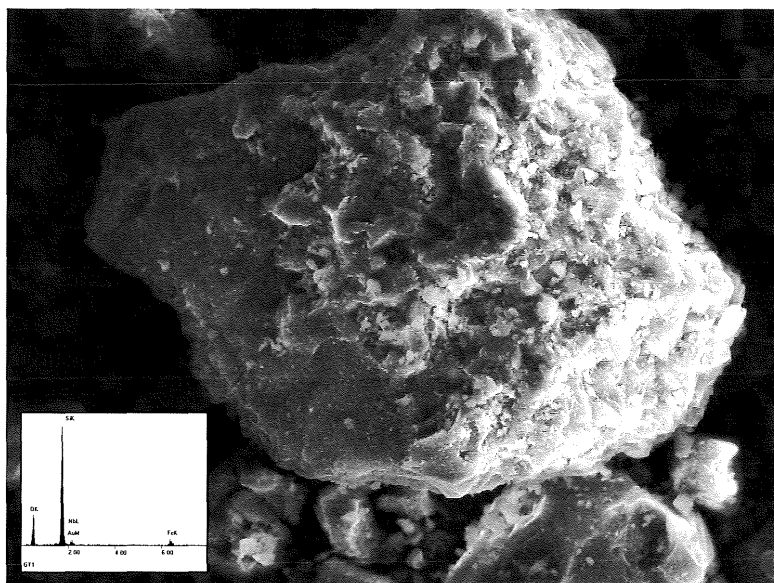
#### DISCUSSION

The microscopic and mineralogical analyses of the GT representative samples allowed to describe all the different typical textures of GT:

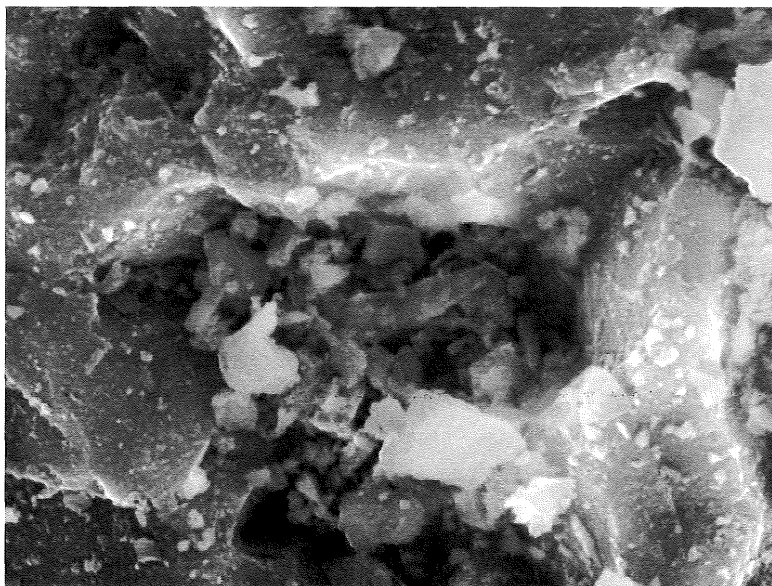
(a) *laminar or laminated*: in sample CTH1

and CTh6 characterized by the overlap of thin layers of quartz crystals and layers with different concentration of iron containing phases yielding different colors (Fig. 7A). The quartz crystals have very small dimensions of about 10-15  $\mu\text{m}$ . Quartz is sometimes accompanied by iron hydroxide massive concentrations distributed along the grain borders. This layered texture is originated by direct sedimentation of the Eocene material mainly composed of small quartz crystals about 10-15  $\mu\text{m}$ . Quartz is sometimes accompanied by iron hydroxide massive concentrations distributed along the grain borders. This layered texture is originated by direct sedimentation of the Eocene material mainly composed of small quartz crystals inside the karstic cavities. No alteration has occurred and the percolating solution rich in iron allowed the re-crystallization of goethite as the cement of the quartz grains.

Fig. 8A is a back-scattered electron image showing the peculiar textural relationship between quartz and goethite and Fig. 8B reports the relative EDS spot analyses. Some nearly idiomorphic quartz crystals do not show

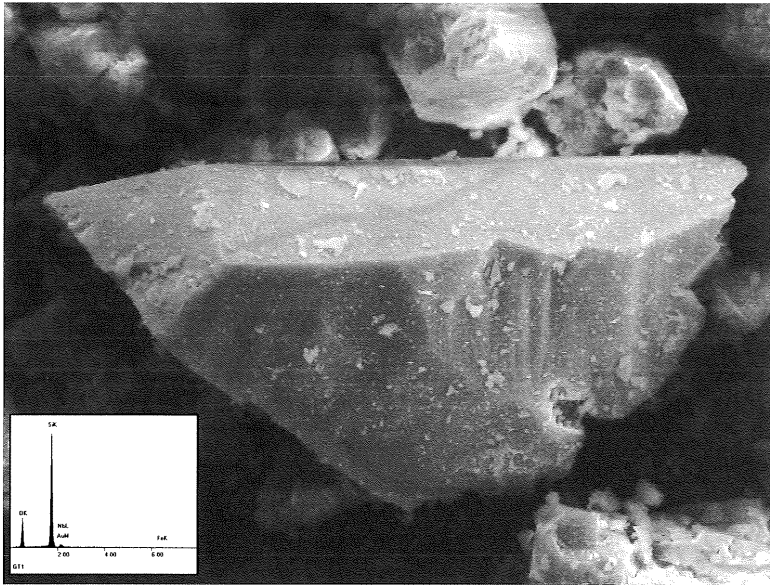


— 20 μm. Sed 25 Kv 750 x A



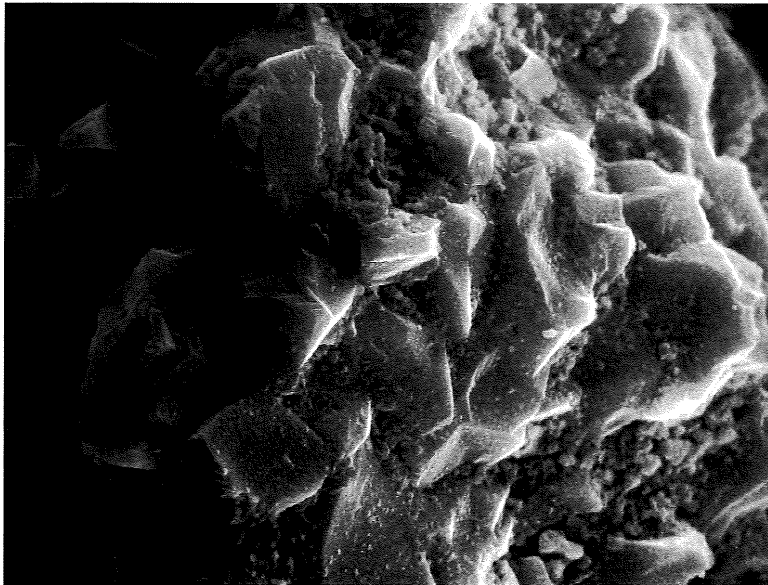
— 2 μm. Sed 25 Kv 6010 x B

Fig. 6 – Secondary electrons (SE) SEM images of CTh1 showing the morphological relationships existing between quartz and goethite. A quartz grain is covered by an agglomerate of smaller crystals corresponding to iron oxides (A). A highly magnified image of the previous one evidenced a tiny cavity entrapping small crystal fragments of quartz and of iron oxides (B).



10  $\mu$ m. Sed 20 Kv 1220 x

C



10  $\mu$ m. Sed 25 Kv 2500 x

D

Fig. 6 – (C). Again the quartz aggregates are cemented by iron oxides (presumably goethite) in (D).

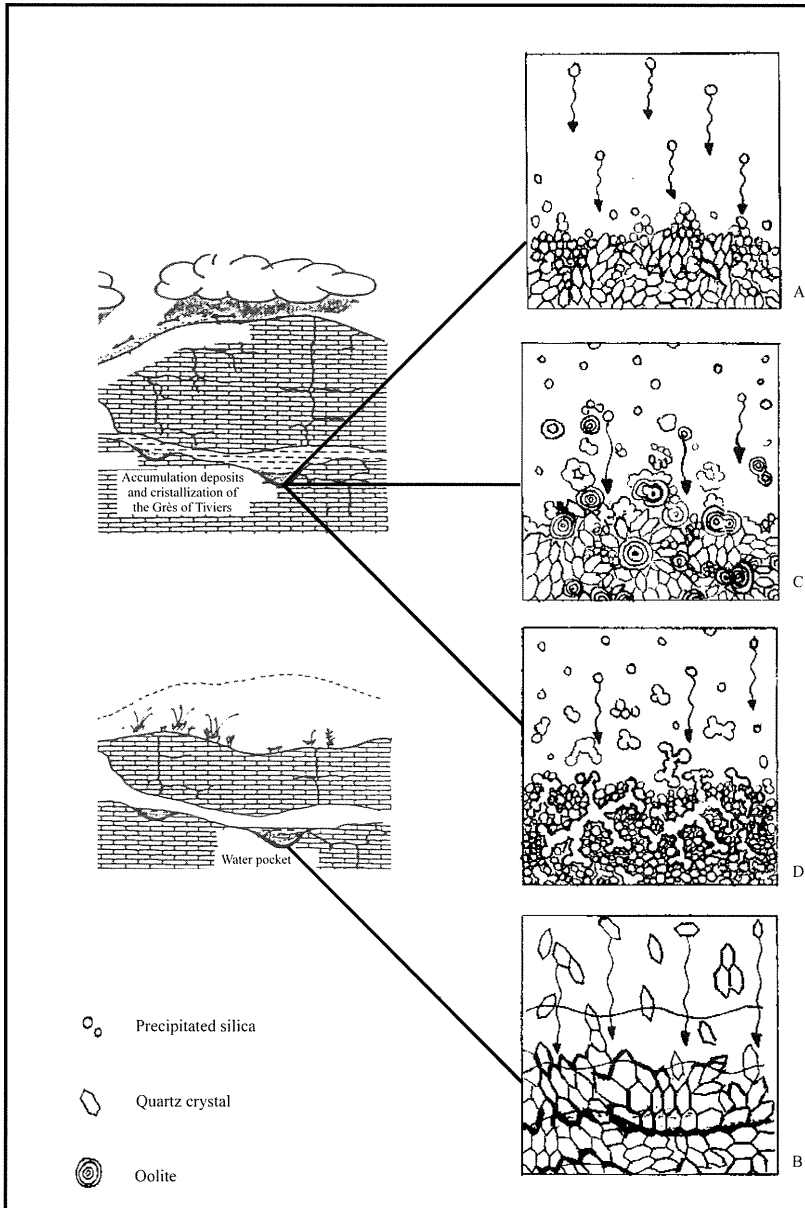


Fig. 7 – Formation of the different microtextures and mineralization of the GT. The layered texture is originated by direct sedimentation of the Eocene material mainly composed of small quartz crystals inside the karstic cavities (A). The homeoblastic texture is formed as a consequence of the percolating waters bearing silica and iron in solution concentrated in a low energy environment where the amorphous silica was precipitated first and in turn transformed into quartz (B) accompanied by re-crystallization of goethite as cement of the quartz grains. The oolitic texture (C) is formed in the same environment of formation of the homeoblastic texture with a different concentration of silica in solution (ppm  $\text{SiO}_2$ ). The dendritic texture origin is secondary as a cementing matrix of the original sedimentary Eocene material mainly composed of small quartz crystals concentrated inside the karstic cavities (D).



iron whereas other crystals are actually aggregates cemented by goethite. It is possible to say that goethite does not form a grain coating on the quartz but on the contrary, it is the cement of the quartz grains.

(b) *homeoblastic*: is displayed by samples CTh3 and CTh6 with a mosaic of quartz crystals having the same average size of 200  $\mu\text{m}$ . The color of the section varies from clear yellow to ochre to the brown-dark according to the concentration of newly-formed cementing goethite. The quartz crystals are secondary. In fact, the microscopic analysis with the polarized light clearly evidenced triple points in correspondence of the junctions among the crystals. In this context, the percolating waters bearing silica and iron in solution have concentrated in a low energy environment where the amorphous silica was precipitated first and in turn transformed into quartz. This process was accompanied by re-crystallization of goethite (sin-genetic or post-genetic is hard to say) as cement of the quartz grains (Fig. 7C).

(c) *oolitic*: displayed by sample CTh8 exhibiting circular concretions of ca. 400  $\mu\text{m}$  diameter originally constituted by opal later transformed into quartz and clustered inside a brownish crystalline matrix. The oolites (ooids) have a transparent core and an onion like microstructure which progressively turns yellow-dark in color towards the boundaries (Fig. 5C). The hypothesis of formation of these oolites implies that the opal concentric crystallization takes place in a low energy environment, far from the detrital contribution (Cornell and Schwertmann, 1996). The accumulation of iron as  $\text{Fe}^{3+}$  oxide, often occurring around a detrital core, is driven by local gradients in the redox potential which is locally higher (Cornell and Schwertmann, 1996).

During the diagenesis, the iron solubility fluctuations allowed the formation of different concentration of iron hydroxides forming the onion like microstructure around the primary nuclei. The environment of formation is similar to that of the homeoblastic texture (Fig. 7C). Here, the concentration of silica in solution

(ppm  $\text{SiO}_2$ ) was much higher and opal oolites formed first. In fact, the solubility of amorphous silica is much higher than the solubility of quartz silica and the precipitation of opal in place of quartz is probably due to the more internally-structured nature of quartz which would require slow precipitation from less concentrated solutions (Berner, 1971; Krauskopf, 1979; Rimstidt and Barnes, 1980). Later, the variation in the silica concentration in solution allowed the re-crystallization of quartz in place of opal. Thus, it is possible to draw two different reaction paths for the formation of homeoblastic texture (precipitation of amorphous silica  $\Rightarrow$  quartz) and for the oolitic texture (precipitation of amorphous silica  $\Rightarrow$  CT-opal  $\Rightarrow$  quartz). The presence of  $\text{Fe}^{3+}$  in solution is invoked for the formation of opal instead of quartz from amorphous silica. In fact, it reacts with  $\text{H}_4\text{SiO}_4$  to form complexes and to increase the solubility of silica (Dove and Rimstidt, 1994) and its concentration favoring the formation of opal. The chemical analysis supports this explanation, sample CTh8 with oolitic texture has the lowest content of  $\text{Fe}_2\text{O}_3$  (3.2 wt%). The lowest the iron content, the higher the probability not to saturate the solution and to precipitate.

The literature reports other siliceous-ferrous concretion deposits with an oolitic texture: in the case of Agbaja Phanerozoic Ironstone Formation (basin of Nupe, Nigeria) oolites containing quartz, goethite and kaolinite were observed. The oolites would be formed by mechanical aggregation originated from the layer-like kaolinite crystals followed by the wavy motion on the water's edge. The goethite would be of post-diagenetic origin and it would be formed by the ferritization of the kaolinitic precursory in a reducing environment (Mücke *et al.*, 1999). Schwarz and Germann (1993) studied the oolitic ironstones of North Sudan and explained the formation of continental oolites by relating the high  $\text{Al}_2\text{O}_3$  content to lateritic processes that involved the sediments as a consequence of the continental complex erosion. This explanation does not hold here

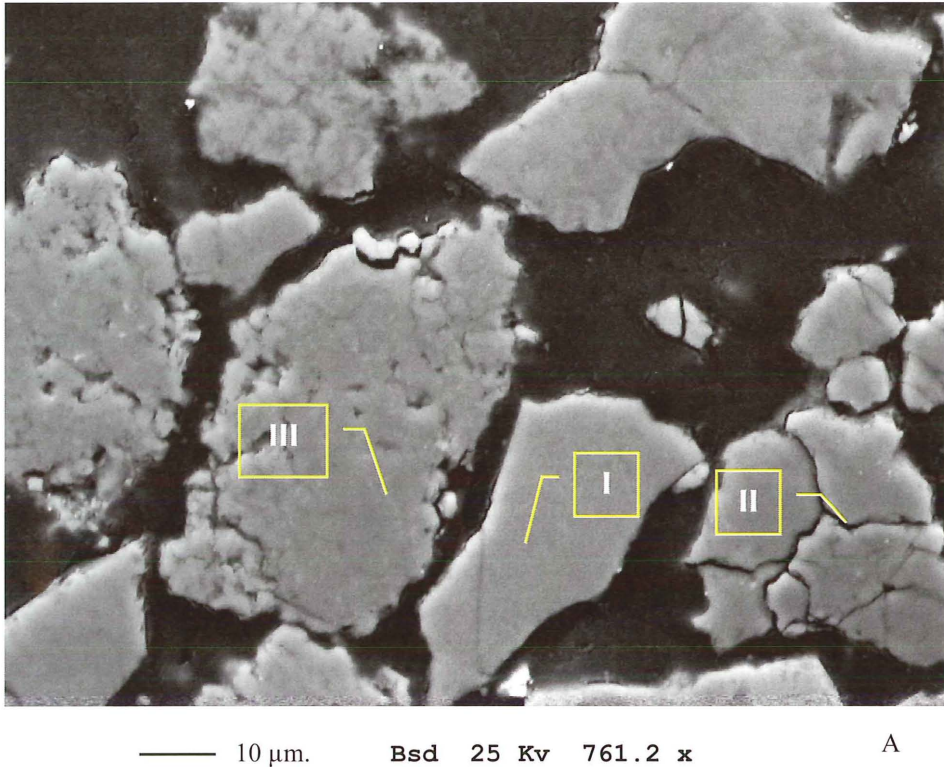
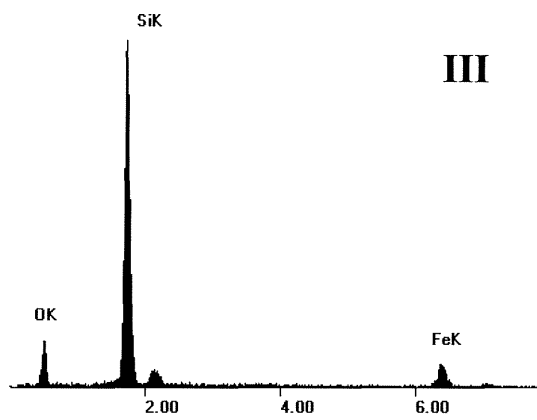
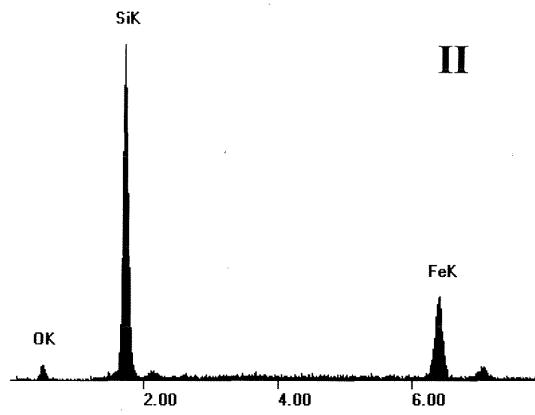
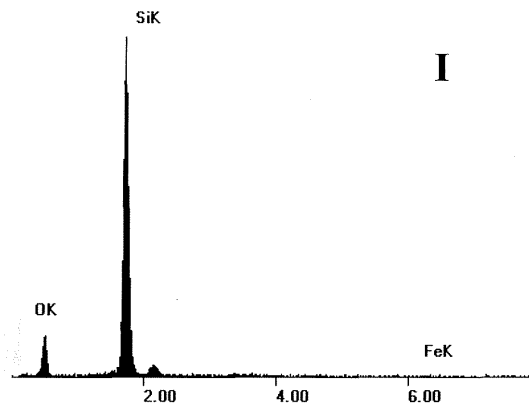


Fig. 8 – Back scattered electrons (BSD) SEM image (see text for details) showing the coarse fraction of the GT (average diameter within 63 and 125  $\mu\text{m}$ ) cemented by an epoxy resin and polished. The relative EDS data are reported in (B).

because unlike the Sudan ironstones oolites, the  $\text{Al}_2\text{O}_3$  content in the GT samples is always less than 1 wt% so that a lateritic origin can be excluded for GT. Another possible setting is described in the Hussainiyat ironstones deposit genesis (West Desert, Iraq) where the presence of oolites containing iron hydroxides, kaolinite and quartz was observed. In this case, the authors attributed the ferrous concretions formation to the action of bacteria in the kaolinitic silt. These structures formed by thin layers of goethite that alternate concentrically to those of kaolinite would be due to Eh periodic fluctuations (Yakta, 1981). Therefore, the nature of these oolitic laminations would suggest a primary formation and not a diagenetic segregation (Al-Bassam and Tamar-Agha, 1998).

(d) *dendritic-like*: observed in sample CTh7 and earlier reported by Thiébaud and Wackenheim (1999) is characterized by quartz crystals nearly equidimensional (200-300  $\mu\text{m}$ ) with a dendritic-like micro-structure corresponding to the goethite concentrations around the idiomorphic quartz crystals. The origin of this microcrystalline phase is secondary as a cementing matrix of the original crystals nearly equidimensional (200-300  $\mu\text{m}$ ) with a dendritic-like micro-structure corresponding to the goethite concentrations around the idiomorphic quartz crystals. The origin of this microcrystalline phase is secondary as a cementing matrix of the original sedimentary Eocene material mainly composed of small quartz crystals concentrated inside the karstic cavities (Fig. 7D). Dendritic-like patterns are generally formed from colloidal solutions either in the form of gel structures, fibrous or microcrystalline aggregates derived by the transformation of initial gels (Stylianou-Savvas, 1995). A typical example is psilomelane formed from Mn-rich



B

gels. Here, the colloidal solution is Fe-rich and the dendritic-like pattern was probably composed of ferrihydrite, lepidocrocite or amorphous iron hydroxides which in turn transformed into goethite.

The results of the analyses of the GT samples (Table 1) evidence a large variability. Regarding the chemical data, SiO<sub>2</sub> has a content ranging from 64.8 wt% in sample CTh6 to 95.2 wt% in sample CTh8 and an obvious inverse relationship exists between the Fe<sub>2</sub>O<sub>3</sub> and SiO<sub>2</sub> contents: the maximum value is reached in sample CTh6 (29.0 wt%) whereas the lowest is exhibited by sample CTh8 (3.2 wt%). Regarding the content of the other oxides, they can be considered impurities. The chemical data are confirmed by the results of the QPA: quartz is the main phase (from 54.9 wt% in sample CTh6 to 82.2 wt% in sample CTh8). Oppositely, goethite ranges from 1.6 wt% in sample CTh8 to 19.8 wt% in sample CTh6.

If the quantity of amorphous phase is plotted versus the percentage of SiO<sub>2</sub>, it is clear that there is no relationship and that the quantity of amorphous phase is nearly constant. Of course, the same observation holds for Fe<sub>2</sub>O<sub>3</sub> which is related to the SiO<sub>2</sub> content. Hence, the amorphous phase seems to be independent from the chemical factors and represents the residual phase during the diagenesis process of GT. The results of the QPA and stoichiometric calculations show that the amorphous fraction of all GT samples is partly composed of silica and partly of iron oxides/hydroxides. It is probably not a coincidence that in the oolitic sample CTh8 the amorphous fraction is just composed of silica as it was likely the opal original precipitate residue.

It is important to remark that part of the amorphous fraction may be due to the grinding process. In fact, it is well known that grinding quartz to micronic size may cause the formation of amorphous silica (Rieck and Koopmans, 1964).

As far as the iron compounds are concerned, it is interesting to comment that hematite is nearly absent in these deposits. GT samples

invariably show goethite and an amorphous phase which is partly composed of (amorphous) iron hydroxides. Although not observed here, it is not possible to exclude that ferrihydrite is the first phase formed from the iron saturated solution. Different reaction pathways are possible and may simultaneously occur if small local chemical variations take place: precipitation of an amorphous precursor⇒goethite; precipitation of an amorphous precursor⇒ferrihydrite⇒goethite; direct precipitation of goethite (under such conditions pH must be very low). In any case, goethite⇒hematite transformation is not observed as well as ferrihydrite⇒hematite transformation. This yields some indications on the chemical environment of formation of the deposits: pH was >3, the concentration of Fe<sup>3+</sup> was not excessive (Fe/O≅0.5), the water activity was ≥1 and in general the dry and warm climatic conditions favoring the goethite⇒hematite transformation were never achieved (Cornell and Schwertmann, 1996).

The presence of nontronite in the CTh4 sample, although purely speculative, is not a surprise because the type locality (Saint-Pardoux, Notron, Dordogne) is only about 30 Km away from the investigated area and nontronite is common in sedimentary iron ore deposits (Simoncoincon *et al.*, 1997).

## CONCLUSIONS

The Grès of Thiviers (GT) is a unique quartz-ferriferous sandstone from the Périgord region in southwestern France, employed as red pigment for traditional ceramics. The typical textures of GT and their genesis were described. The most frequent texture is the laminar one, due to the overlap of beds formed by small quartz crystals and beds of iron hydroxides. Other less frequent textures are: oolitic, with circular opal concretions engulfing the iron oxide particles; dendritic, homeoblastic with different sizes of the quartz crystals and form of the goethite concretions. The presence of amorphous phase was discovered in all

samples and related to the fraction of silica and iron oxides that were not crystallised into quartz and goethite.

On the basis of the chemical and mineralogical analyses, GT was shown to be invariably composed of quartz, goethite and amorphous phase in variable proportions. The SEM observations allowed the interpretation of the morphological phase relationships showing that the quartz crystals are mainly cemented by goethite.

Chemical and quantitative mineralogical phase compositions were related to the textural characteristics and can be very useful for the search of the material with the best quality to produce the red ceramics. In fact, the material with quartz as cement of the goethite phase (like in the homeoblastic texture displayed by sample CTh3) is also the one with the best yield in terms of red colour in firing. Both the oolitic (sample CTh8) and the dendritic (CTh7) textures are not good for the industrial applications. In the oolites, the silica/goethite ratio is too high and the colouring power is low. Oppositely, in the dendrites, goethite is in excess and not protected by the quartz grains. It is difficult to say *a priori* if the laminar texture (sample CTh1) is invariably good for the industrial applications because the colouring yield is dependent on many factors such as the thickness of the layers, the presence of iron rich layers with uncoated amorphous iron hydroxides, the silica/coated or embedded goethite.

#### ACKNOWLEDGMENTS

Dr. M. Tonelli is acknowledged for help during the SEM sessions at the C.I.G.S. laboratory of the University of Modena and Reggio Emilia. Dr. P. Venturelli is also greatly acknowledged for help in the experimental part. Thanks to CESAR, société du groupe IMERYS, ST Sulphice de Mareuil, France. We also acknowledge Denain-Anzin Minéraux Société (St-Jean De Cole, France) for help in the sampling activity and for making available pictures from a private communication by Thiébaud and Wackenheim (1999) of their property. Si ringraziano infine i due (tre?) referees anonimi per le giuste critiche e l'aiuto nella revisione del manoscritto.

#### REFERENCES

- AL-BASSAN, K.S and TAMAR-AGHA, M.Y. (1998) — *Genesis of the Hussainiyat ironstone deposit, Western Desert, Iraq*. Mineral. Dep., **33**, 266-282.
- BERNER, R.A. (1971) — *Principles of Chemical sedimentology*. McGraw-Hill, New York, pp. 256.
- CORNELL, R.M. and SCHWERTMANN, U. (1996) — *The iron oxides*. VCH, Weinheim, pp. 573.
- DORNIEDEN, TH., GORBUSHINA, A.A., and KRUMBEIN, W.E. (2000) — *Biodecay of cultural heritage as a space/time-related ecological situation – an evaluation of a series of studies*. International Biodeterioration and Biodegradation, **46**, 261-270.
- DOVE, P.M. and RIMSTIDT, J.D. (1994) — *Silica-water interactions* in: Silica physical behavior, geochemistry and materials applications. Reviews in Mineralogy **29**, P.J. Heaney, C.T. Prewitt and G.V. Gibbs eds. Mineral. Soc. Am., 259-301.
- DUBREUILH, J. (1980) — *Carte géologique de la France (1/50000), feuille Montguyon (756) et notice explicative BRGM*.
- DUBREUILH, J. (1982) — *Carte géologique de la France (1/50000), feuille Coutras (780) et notice explicative BRGM*.
- DUBREUILH, J. (1984) — *Carte géologique de la France (1/50000), feuille Belvès (831) et notice explicative BRGM*.
- DUBREUILH, J. (1989) — *Synthèse paléogéographique et structurale des dépôts fluviaux tertiaires du nord du bassin d'Aquitaine. Passage aux formations palustres, lacustres et marines*. Documents BRGM.
- EGGLETON, R. (1977) — *Nontronite: chemistry and X-ray diffraction*, Clay Minerals, **12**, 181-194.
- GERSAL, F. (1998) — *The discovery of the Lascaux caves*. Historia, **619**, 108-109.
- GOURDON-PLATEL, N. (1975) — *Les minerais de fer en Aquitaine et leur intérêt historique*. Bulletin Société Linneau Bordeaux, **V**, 33-47.
- GOURDON-PLATEL, N. (1977) — *Hypothèses sur la formation des dalles silico-ferrugineuses de la bordure Nord-Aquitaine*. Géomorphology Dynamics, **2**, 59-65.
- GUALTIERI, A.F. (2000) — *Accuracy of XRPD QPA using the combined Rietveld-RIR method*. J. Appl. Crystallography, **33**, 267-278.
- LARSON, A.C. and VON DREELE, R.B. (1994) — Los Alamos National Laboratory Report LAUR 86-748.
- KRAUSKOPF, K.B. (1979) — *Introduction to Geochemistry*. McGraw-Hill, New York, pp. 617.
- MASSET, C. (1997) — *Men during the time of Lascaux, 40000-10000 BC*. Homme, **37(142)**, 171.
- MÜCKE, A., BADEJOKO, T. A. and AKANDE, S.O. (1999) — *Petrographic-microchemical studies and*

- origin of the Agbaja Phanerozoic Ironstone Formation, Nupe Basin, Nigeria: a product of ferruginized ooidal kaolin precursor not identical to the Minette-type.* Mineral. Dep., **34**, 284-296.
- PLATEL, J.P. (1980) — *Carte géologique de la France (1/50000), feuille Barbezieux (732) et notice explicative* BRGM.
- PLATEL, J.P. (1981) — *Carte géologique de la France (1/50000), feuille Montmoreau (733) et notice explicative* BRGM.
- PLATEL, J.P. (1983) — *Carte géologique de la France (1/50000), feuille Fumel (855) et notice explicative* BRGM.
- PLATEL, N. and DUBREUILH, J. (1992) — *Les ferruginisations et les argiles associées au Paleokarst tertiaire du Périgord (Dordogne, France). Karst et évolutions climatiques.* Presses Universitaires de Bordeaux, 449-460.
- RIECK, G.D. and KOOPMANS, K. (1964) — *Investigation of the disturbed layer of ground quartz.* Brit. J. Appl. Phys., **15**, 419-425.
- RIMSTIDT, J.D. and BARNES, H.L. (1980) — *The kinetics of silica-water reactions.* Geochim. Cosmochim. Acta, **44**, 1683-1699.
- SCHWARZ, T. and GERMANN, K. (1993) — *Ferricretes as a source of continental oolitic ironstones in northern Sudan.* Chem. Geol. **107**, 259-265.
- SEMPIO, A. and GUALTIERI, A.F. (2001) — *Utilizzo del Grès di Thiviers nel grès porcellanato.* Ceramurgia, **4**, 97-110.
- SIMONCOINCON, R., THIRY, M. and SCHMITT, J.M. (1997) — *Variety and relationships of weathering features along the Early Tertiary palaeosurface in the Southwestern French Massif Central and the nearby Aquitaine basin.* Palaeogeography, Palaeoclimatology, Palaeoecology, **129(1-2)**, 51-77.
- STYLIANOS-SAVVAS, P.A. (1995) - *Atlas of the textural patterns of ore minerals and metallogenic processes.* De Gruyter Editor, New York, pp. 659.
- THIÉBAUT, J. and WACKENHEIM, C. (1999) — *Études micrographiques d'échantillons de roches silico-ferrugineuses du Périgord.* Private communication Université de Franche Comté.
- YAKTA, S. A. (1981) — *Ironstone sedimentation in the Western Desert, Iraq.* MSc Thesis University of Wales.